

Evaluating the efficiency of the observation system to recover the tsunami source by the r -solution method

Tatyana Voronina

Abstract. In this study, the tsunami source of the 2013 Solomon Island tsunami event was reconstructed by the r -solution method. The focus of this research is the applying the regularities obtained for a model cases to the real event. To understand the reasonable strategy of deployment of a tsunami recorders, series of the numerical experiments were carried out and DART Buoys monitoring system, for the case in question, was examined for the efficiency to infer the tsunami source. The method proposed suppresses the negative effect of the ill-posedness of the problem determining the inevitable instability of the numerical solution.

Introduction

Tsunamis are very long gravity waves, with wavelengths of tens to hundreds kilometers, which exceed the ocean depth. Under such conditions, in the deep ocean their propagation can be described by the shallow-water theory. Tsunamis can be triggered by a variety of geophysical phenomena. In the first and more common case, an earthquake occurred near the sea floor, may produce a co-seismic deformation that can cause a displacement in the sea floor that can, in turn, cause an initial sea surface deformation that may result in a tsunami wave. To accurately forecast the inundation and run up in the near-field coast, where a warning should be issued no more than 20 minutes, it is necessary to gain the insight into a tsunami source at the early stages of tsunami propagation.

Numerous studies deal with application of tsunami waveforms inversion for determining the tsunami source characteristics [1–10].

The tsunami waveform inversion has the advantage in determining a tsunami source, as compared with seismic waveform inversion because seismic data are often imprecisely translated into tsunami data. Furthermore, the tsunami wave propagation can be more accurately simulated than seismic waves due to the fact that bathymetry is better known than subsurface seismic velocity structure.

Presently, a lot of offshore tsunami monitoring systems using submarine cabled seafloor observatory technology have been deployed in the deep ocean. One of them is the Deep-ocean Assessment and Reporting of Tsunamis

(DART) buoy system developed by the Pacific Marine Environmental Laboratory of the National Oceanic Atmospheric Administration [11]. The tsunami waveforms acquired by cabled offshore ocean bottom tsunami meters are more available, free of the tide gauge response functions as well as the coastal and the harbor effects. Hence, the inversion approaches based on the deep-ocean observations can be used for a rapid estimation of a tsunami source, which, in turn, can be used as direct input for the real-time forecast of the tsunami impact.

This study proposes an application of an inversion method for reconstructing a tsunami source by using the tsunami waveforms recorded by DART Buoys of February 6, 2013 during Solomon Islands Tsunami. The technique based on the least-squares inversion using the truncated Singular Value Decomposition (SVD) and r -solution methods [12] has been already described in its fundamentals in [13, 14].

Noisiness of the real data presents a major obstacle in applying the mathematical technique to the inverse problem in reality. The inverse problem in question is treated as an ill-posed problem of the hydrodynamic inversion with tsunami waveforms, so, this is the cause of the inevitable instability of the numerical solution. The method presented allows one to control the instability of the numerical process and to obtain an acceptable result in spite of the ill-posedness of the problem.

Although a considerable attention has been given to developing the inversion methods to infer the initial tsunami waveform, a lesser number of studies has been devoted to revealing the influence of such characteristics of the monitoring system as the number and spatial distribution of the recording devices on the inversion results. In order to correlate these notions, a series of numerical experiments with synthetic data and different computational domains have been carried out in previous studies. The results have been presented in [15, 16].

The focus of this research is on applying the regularities obtained for a more reasonable strategy of deployment of a tsunami monitoring system in reality. Results of numerical experiments are presented in the case study of Solomon Islands tsunami of February 6, 2013.

1. Model

The tsunami wave is assumed to be triggered by a sudden vertical displacement of the sea floor. The tsunami propagation can be considered within of shallow-water theory. The tsunami source area is assumed to be known from the seismological data as a rectangle Ω , $\Omega \subset \Phi \subseteq \Pi$, where a rectangular domain Π is a calculation domain and Φ is the aquatic part of Π with the piecewise-linear solid boundaries Γ and straight-line sea boundaries. The problem is considered in an orthogonal coordinate system. The

plane $\{z = 0\}$ corresponds to the undisturbed water surface. The curvature of the Earth is neglected. The wave run up is not considered.

Let $\eta(x, y, t)$ be a function of the water surface elevation relative to the mean sea level which is considered to be a solution of the linear shallow-water equations

$$\eta_t + g\nabla \cdot (h\vec{V}) = 0, \quad \vec{V}_t + g\nabla\eta = 0 \quad (1)$$

with the initial conditions

$$\eta|_{t=0} = \varphi(x, y), \quad \vec{V}|_{t=0} = 0, \quad (2)$$

the boundary condition on the solid boundary

$$\vec{V} \cdot \vec{n} = 0, \quad (3)$$

as well as absorbing boundary conditions (ABC) of second order of accuracy implied at the sea boundaries on the sides of the rectangle Π :

$$\begin{aligned} c\eta_{yt} - \eta_{tt} + \frac{c^2}{2}\eta_{xx}\Big|_{y=0} &= -c\eta_{yt} - \eta_{tt} + \frac{c^2}{2}\eta_{xx}\Big|_{y=Y} = 0, \\ -c\eta_{xt} - \eta_{tt} + \frac{c^2}{2}\eta_{yy}\Big|_{x=X} &= c\eta_{xt} - \eta_{tt} + \frac{c^2}{2}\eta_{yy}\Big|_{x=0} = 0. \end{aligned} \quad (4)$$

In the above equations, $\vec{V} = (v_x, v_y)$ is the horizontal fluid velocity vector, $h(x, y)$ is the water depth relative to the mean sea level, g is the gravity acceleration, $c(x, y) = \sqrt{gh(x, y)}$ is the wave phase velocity, \vec{n} is the outer normal unit vector to the boundary, and $\varphi(x, y)$ is the initial water displacement defined in the tsunami source area Ω .

2. Inversion method

The inverse problem at hand is to infer the unknown initial water displacement $\varphi(x, y)$ as output while the observed tsunami waveforms as data input are assumed to be known on a set of points $R = \{(x_i, y_i), i = 1, \dots, P\}$ (below called as receivers):

$$\eta(x_i, y_i, t) = \eta_0(x_i, y_i, t), \quad (x_i, y_i) \in R. \quad (5)$$

This inverse problem is treated as an ill-posed problem of the hydrodynamic inversion with tsunami sea-level records, so it imposes some restrictions on the use of mathematical techniques. In the approach applied, regularization is performed by means of the truncated SVD that brings about the notion of r -solution (see [12]). This solution will be sought for in a least squares formulation. The application of this approach to tsunami waveforms inversion was in detail described in [15, 16].

The unknown function of the water surface displacement $\varphi(x, y)$ in the source area Ω was sought for as a series of spatial harmonics

$$\varphi(x, y) = \sum_{m=1}^M \sum_{n=1}^N c_{mn} \sin \frac{m\pi}{l_1} x \cdot \sin \frac{n\pi}{l_2} y \quad (6)$$

for $(x, y) \in [0, l_1] \times [0, l_2]$, with unknown coefficients $\vec{c} = \{c_{mn}\}$.

In our case, the inverse problem data are the observed waveforms (*marigrams*) $\vec{\eta} = (\eta_{11}, \dots, \eta_{1N_t}, \eta_{21}, \dots, \eta_{2N_t}, \eta_{P1}, \dots, \eta_{PN_t})^T$, $\eta_{pj} = \eta(x_p, y_p, t_j)$, on the set of points (x_p, y_p) , $p = 1, \dots, P$, and at time instants t_j , $j = 1, \dots, N_t$. Then the vector $\vec{\eta}$ containing the observed tsunami waveforms can be expressed as follows:

$$\vec{\eta} = \mathbf{A}\vec{c}, \quad (7)$$

where \mathbf{A} is a matrix which columns consist of computed waveforms for every spacial harmonic $\varphi_{mn}(x, y) = \sin \frac{m\pi}{l_1} x \cdot \sin \frac{n\pi}{l_2} y$ used as the initial condition to the direct problem (1)–(4). The coefficients α_k of decomposition of vector \vec{c} to the right singular vectors $\vec{c} = \sum_{j=1}^{MN} \alpha_j \vec{e}_j$ are expressed as follows $\alpha_j = \frac{(\vec{\eta}, \vec{l}_j)}{s_j}$, where \vec{l}_j and \vec{e}_j are the left and the right singular vectors of the matrix \mathbf{A} and s_j are its singular values. Then, the r -solution of equation (7) is represented as $\vec{c}^{[r]} = \sum_{j=1}^r \alpha_j \vec{e}_j$ and, finally, the desired function $\varphi(x, y)$ takes the form

$$\varphi^{[r]}(x, y) = \sum_{j=1}^r \alpha_j \sum_{m=1}^M \sum_{n=1}^N \beta_{mn}^j \varphi_{mn}(x, y), \quad (8)$$

where $\vec{e}_j = (\beta_{11}^j, \dots, \beta_{MN}^j)^T$. The solution obtained is stable for any fixed r with respect to perturbations of the right-hand side. The relationship between r and the singular values of the matrix \mathbf{A} as well as the conditioning number (noted as **cond**) of the matrix obtained by projection of the operator A in equation (7) onto a linear span of its r first right singular vectors can be expressed as $r = \max\{k : s_k/s_1 \geq 1/\mathbf{cond}\}$. Thus, the value of r is determined by the singular spectrum of the matrix \mathbf{A} , and it is still significantly smaller than the dimension of the matrix obtained. A sharp decrease in the singular values, when their numbers increase, is typical for all the calculations, due to the ill-posedness of the problem. Increasing the value r leads therewith to a higher instability. On the other hand, the parameter r should be large enough to provide a suitable spatial approximation of the function $\varphi(x, y)$. It is clear that properties of the matrix \mathbf{A} and, consequently, the quality of the obtained solution are determined by the location and extent of the tsunamigenic area, the configuration of an observation system and the temporal extent of the signal. Some properties of the inverting operator in the context of retrieving a tsunami source were studied numerically in [15].

3. The influence of a tsunami monitoring system location on the inversion results

A series of calculations have been carried out by the method proposed to clarify the dependence of the efficiency of the inversion on certain characteristics of the observation system such as the number of receivers and their location. The inversion method described above was applied to the 2013 Solomon Islands event. The February 6, 2013 magnitude 8.0 Mw Santa Cruz Islands, Solomon Islands earthquake (10.738° S, 165.138° E), depth of 29 km, generated a tsunami that was observed all over the Pacific region and caused deaths and damage locally.

In Figure 1, the domain $\Pi = \{(x; y) : 140^\circ \text{ E} \leq x \leq 185^\circ \text{ E}; 17^\circ \text{ S} \leq y \leq 13^\circ \text{ N}\}$ of tsunami propagation calculated with GEBCO bathymetry (1-min resolution; available at <http://www.gebco.net/>) is presented. We consider a Cartesian coordinate system with the origin at the point (140° E, 17° S). Let the Ox -axis and the Oy -axis be directed along the longitude and latitude accordingly. The tsunami source area is a rectangle $\Omega = \{164.638^\circ \text{ E} \leq x \leq 165.638^\circ \text{ E}; 11.238^\circ \text{ S} \leq y \leq 10.238^\circ \text{ S}\}$. The sea levels were recorded by the system of six ($P = 6$) DARTs marked by the white color (\circ) and enumerated clockwise in Figure 1: 1—55012; 2—55023; 3—52403; 4—52402; 5—52406; 6—51425. The time interval is long enough for the tsunami wave to reach all the receivers, specifically, the time step is 4 s, the number of time steps is $N_t = 2000$. In these calculations the values of parameters M and N

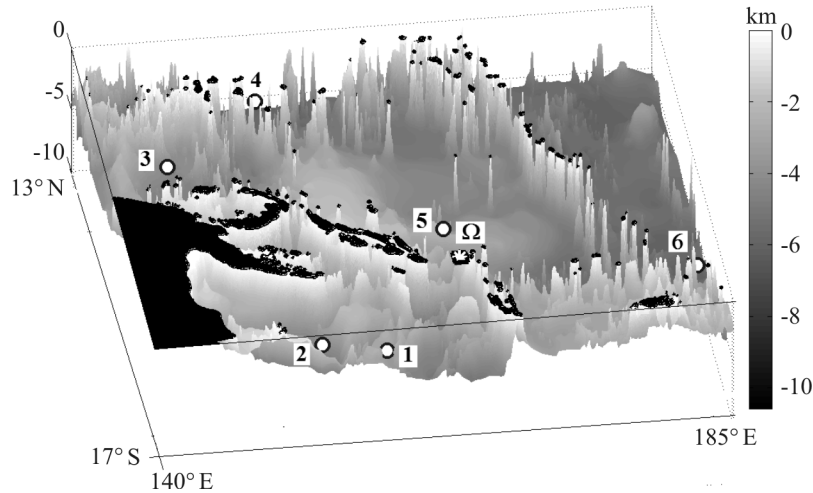


Figure 1. The bathymetry in calculation domain II. DART buoys are marked by the white color symbols (\circ) with their numbers, the target domain is marked by the black rectangle, the epicenter is marked by the white star. The black domain corresponds to dry land

are empirically established as $M = 15$, $N = 15$. The matrix \mathbf{A} is about $(225 \times 2000p)$, where p is equal to the number of tsunami waveforms used in the inversion.

Numerical simulation is based on a finite difference algorithm and the method of staggered grids. Rectangular grids of 2700×1800 and 61×61 nodes were placed over the domains Π and Ω , respectively. The epicenter of the tsunami source is assumed to be at the node $(1509, 376)$. The matrix \mathbf{A} is computed with MOST (Method of Splitting Tsunami) package (<http://nctr.pmel.noaa.gov/model.html>) adopted to NVIDIA GPU [17]. Further, standard SVD-procedure was applied to the matrix \mathbf{A} . The analysis of singular spectrum of the matrix \mathbf{A} allows one to define the number r and to compute the coefficients $\{c_{mn}\}$ as an r -solution of equation (7). After this, the function $\varphi^{[r]}(x, y)$ was computed in the form (8).

The series of the numerical experiments with real data were aimed to highlight the way of varying the observation system on improving inversion. One of the main factors which contribute to the difficulties is the complexity of the bottom relief with a plenty of submarine rocks and chains in the considered domain. Furthermore, it was interesting to obtain an acceptable results of the inversion using a minimum number of observed waveforms. As is known, increasing the number of receivers does not often lead to a good inversion if there is no optimal azimuthal coverage with respect to the source and, on the contrary, in real cases it turns out that the noisiness of data is raised resulting in lowering the efficiency of inversion.

First of all, the singular spectrum of the matrix \mathbf{A} was analyzed in every case. In Figure 2a, common logarithms of singular values of \mathbf{A} are shown for different subsets of the receivers. In Figure 2b, zoomed plots from Figure 2a are presented. Given a fixed bound on the conditioning number

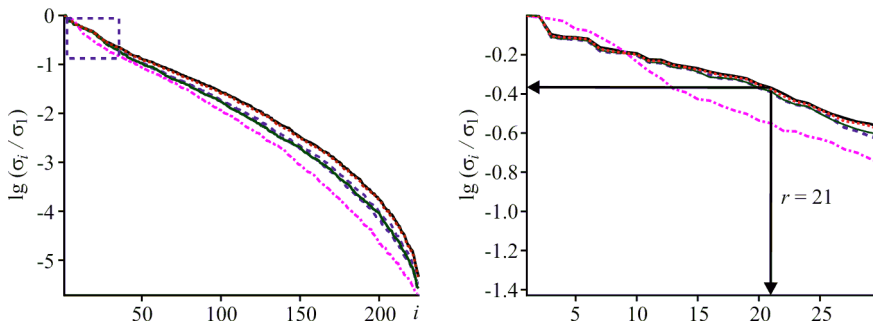


Figure 2. Plots of singular values in the common logarithmic scale of matrix \mathbf{A} with respect to their numbers are marked by the different line styles relative to the receivers used in the inversion: $\{4, 5, 6\}$ (the dashed-dotted line), $\{1, 3, 5\}$ (the dashed line), $\{1, 5, 6\}$ (the thin solid line), $\{1, 2, 3, 5, 6\}$ (the dotted line), and $\{1, 2, 3, 4, 5, 6\}$ (the black line)

one can define value of r as an x -coordinate of the intersection point for the corresponding horizontal line and the singular value plot. Obviously, if the singular value plot decreases more or less smoothly up to some point, there is an opportunity to use larger r and, hence, to obtain more informative solution. For the below considered receiver subsets using $r > 21$ appears to be impracticable due to the high level of the noisiness of the observed data which leads to the solution instability (see such example in Figure 3 below).

Analysis of the singular spectra plays the key role to understand the relationship between the improvement of inversion and a change in the configuration of the observation system. It is clear that modifying in the subset of receivers results in changing the corresponding singular spectrum. Indeed in Figure 2, the dashed line for the subset consisting of Receivers 1, 3, 5 and the dashed-dotted line for the subset consisting of Receivers 4, 5, 6 significantly differ, that is a consequence of the replacement of Receiver 1 by Receiver 4. This is in good agreement with a change in the inversion results presented in Figure 4b, c.

Analysis the plots in Figure 2 makes possible to expect that the worst inversion results would be obtained by using the subset consisting of Receivers 4, 5, 6 due to the more sharp decrease of its singular values in comparison to others. Indeed, comparison of the results presented in Figure 4 confirms this assumption.

As it is shown in Figure 2, the singular spectra of the monitoring systems involving Receivers 1, 3, 5 (the dashed line), 1, 2, 3, 5, 6 (the dotted line), and 1, 2, 3, 4, 5, 6 (the solid line) are similar in appearance. It is possible to expect similar results of the inversion in these cases. The results presented in Figure 3b and in Figure 4b, f confirm this idea. Such sets of receivers provide sufficiently plausible results, as evidenced by comparing the marigrams from this recovered source with observed ones that are presented in Figure 5.

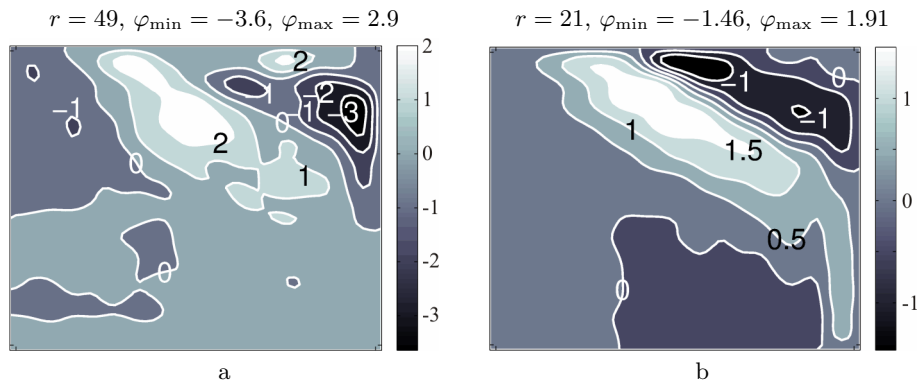


Figure 3. Recovered initial functions in the domain Ω inverted using Receivers 1–6 with different values of r

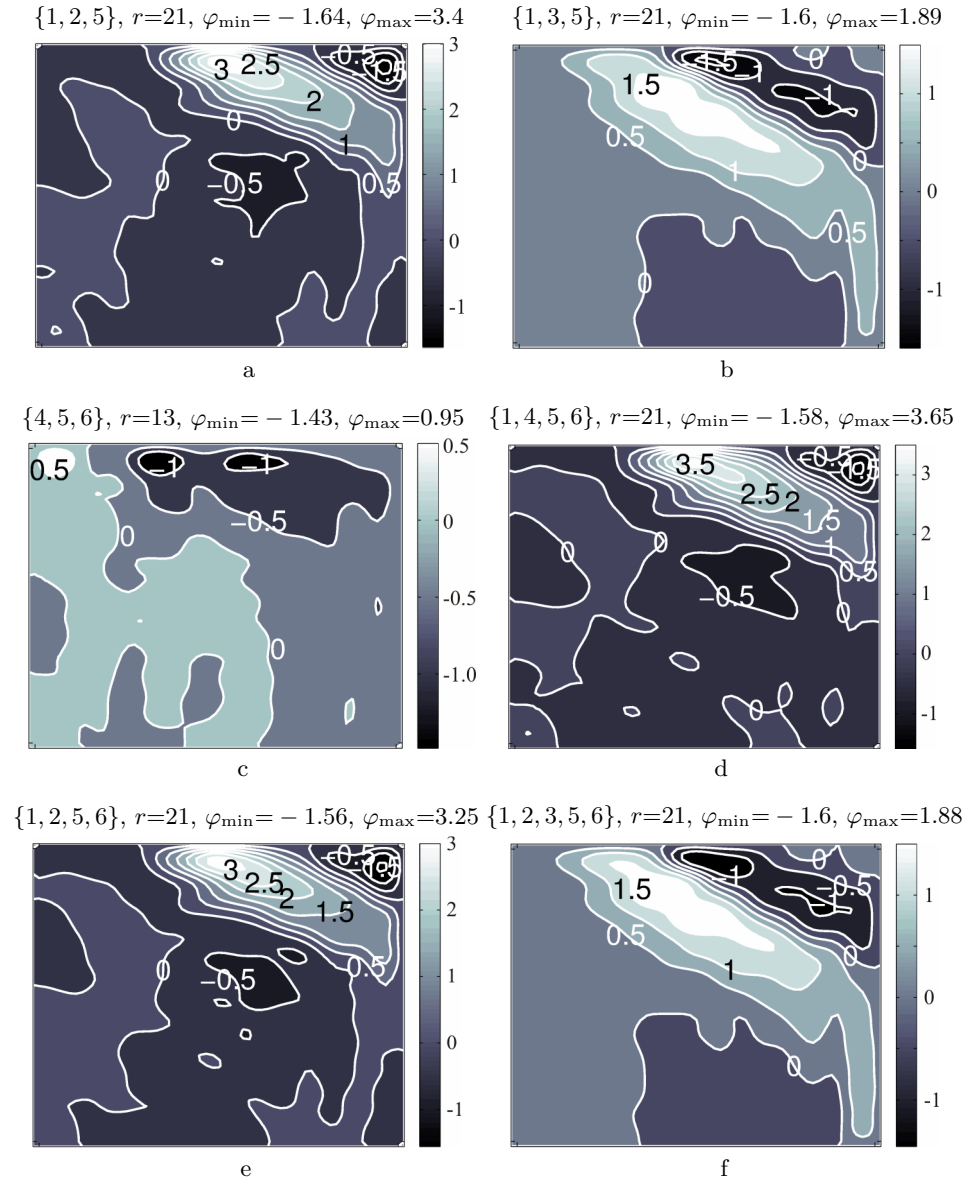


Figure 4. Recovered initial functions in the domain Ω inverted by using different subsets of receivers. The cases with the conditioning number of 2.5 for the matrix obtained are shown. Used receivers are enumerated in braces

The importance of azimuthal coverage with respect to the tsunami source and bathymetry features are illustrated by the inversion results for different receiver sets such as 1, 2, 5 (Figure 4a), 1, 3, 5 (Figure 4b) and 4, 5, 6 (Figure 4c). As is clear from the plots a, b, c in Figure 4, the inversion results for the equipotent subsets and the common **cond** of the matrixes obtained are differ. The results by Receivers 1, 3, 5 is much better than for the subsets 1, 2, 5 and 4, 5, 6. The usage of Receiver 3 and Receiver 1 significantly improve both the shape and the amplitude of the source (the plots in Figure 4a and 4b as well as in Figure 4e and 4f the plots in Figure 4c and 4d). The last can be due to its perfect location in the direction of reflections from the submarine rock trail. On the contrary, a remote Receiver 4, surrounded by the islands, does not have any impact on the solution and, probably, only introduces additive noise. The same conclusion can be made for Receivers 6 and 2 from the comparison the results presented in Figure 4a and 4e, as well as from the comparison the results presented in Figure 4a and 4b. The fact is in our case, a decrease in the length of the records used in the inversion does not make any evidence of a positive effect.

The approach proposed provides a way to balance the number of the receivers and the quality of the inversion. Based on the analysis of a singular spectrum for each specific observation system one can define a maximal r which allows one to avoid the numerical instability.

Indeed, the results of numerical experiments presented in Figure 4 substantiate our assumption based on analyzing singular spectra.

Based on the carried out numerical experiments, it is possible to conclude that the subsets including Receivers 1, 3, 5 are the most efficient to reconstruct the tsunami source by the method proposed.

After the inversion by tsunami waveforms from the Receivers 1, 2, 3, 5, 6 was completed, the direct problem was once again solved with the recovered function $\varphi(x, y)$ as the initial condition (2) and the marigrams were calculated at the same six points, where DARTs Buoys were assumed. As is clear from Figure 5, the marigrams computed with the recovered tsunami source have a sufficient matching with the real data. This result can be improved by special filtration of the observed data.

4. Conclusion

The instability of a numerical solution of the ill-posed inverse problem in question in many instances is due to the noise in real marigrams that is a common feature in any real applications. An approach based on r -solution method allows one to control the instability of a numerical solution and to obtain an acceptable result in spite of ill-posedness of the problem. The method seems attractive from the computational point of view since the

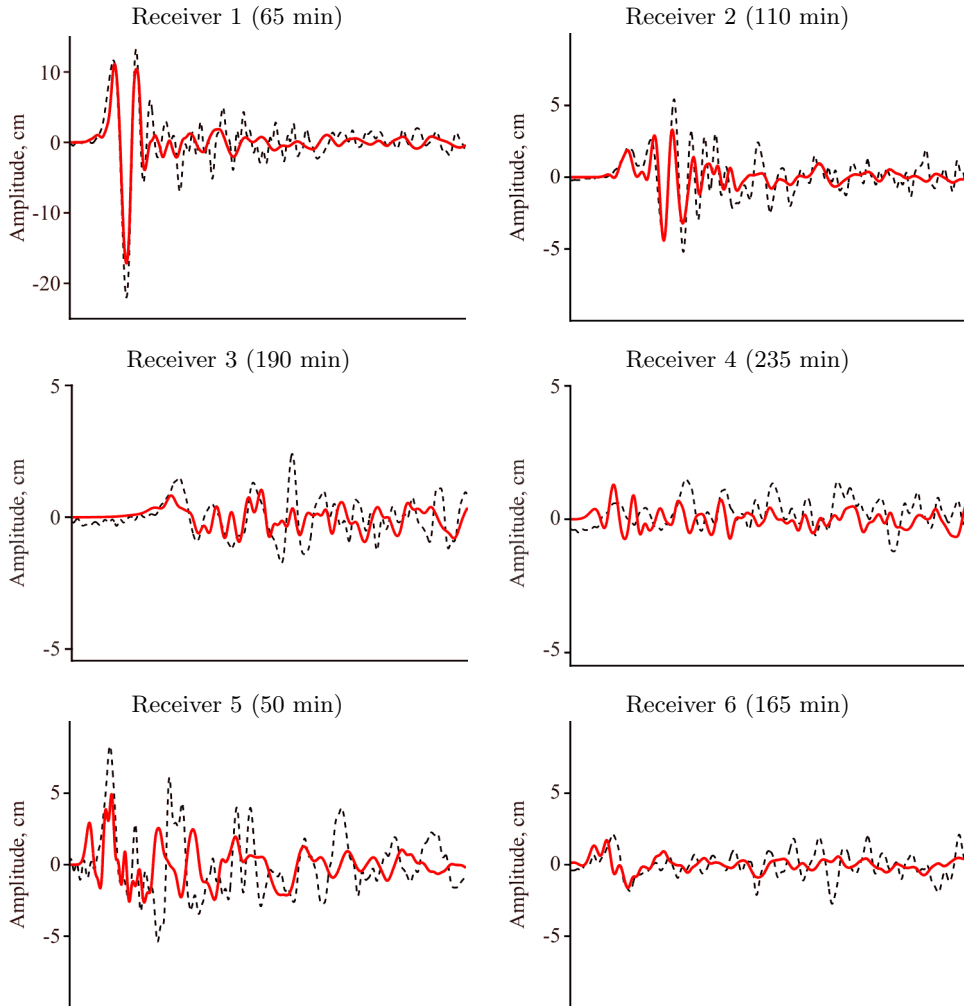


Figure 5. Comparison of the observed tsunami waveforms (dash line) within 130-minute interval and calculated ones (solid line) by using the records of Receivers 1, 2, 3, 5, 6 for the 2013 Solomon Islands event. The starting delay after the earthquake origin time is shown in parentheses

main efforts are required for calculating the matrix \mathbf{A} . If an observation system is fixed and tsunami-prone areas are defined, one can compute the matrix only once as a preliminary stage.

The receiver location effects the choice of the number r in such a way: the better is the configuration of the observation system, the longer is a weakly decreasing part of the spectrum. Thus, the rate of the singular values descent which is most directly correlated with the receiver location should be considered as main parameter of the efficiency of the inversion.

It is possible to make a preliminary evaluation of the efficiency of the inversion with a given set of recording stations by analyzing the singular spectrum of a relevant matrix. The results obtained allow to find the way to improve the inversion by selecting the most informative set of available recording stations. Since tsunami sources have often a dipolar shape, the location of receivers on direct and reflected rays corresponding to the direction of the strongest variability of the dipole source have the greatest effect for the inversion result.

The function recovered by the method proposed can find practical use both as an initial condition for various optimization approaches and for computer calculation of the tsunami wave propagation.

References

- [1] Satake K. Inversion of tsunami waveforms for the estimation of hereogeneous fault motion of large submarine earthquakes: the 1968 Tokachi-oki and the 1983 Japan sea earthquake // *J. Geophys. Res.* — 1989. — Vol. 94. — P. 5627–5636.
- [2] Tinti S., Piatanesi A., Bortolucci E. The finite-element wavepropagator approach and the tsunami inversion problem // *J. Phys. Chem. Earth.* — 1996. — Vol. 12. — P. 27–32.
- [3] Piatanesi A., Tinti S., Pagnoni G. Tsunami waveform inversion by numerical finite-elements Green's functions // *Nat. Hazards Earth Syst. Sci.* — 2001. — Vol. 1. — P. 187–194.
- [4] Pires C., Miranda P.M.A. Tsunami waveform inversion by adjoint methods *J. Geophys. Res.* 2010. — Vol. 106. — P. 19773–19796.
- [5] Titov V.V., Gonzalez F.I., Bernard E.N., Eble M.C., Mofjeld H.O., Newman J.C., Venturato A.J. Real-time tsunami forecasting: Challenges and solutions *Nat. Hazards, Special Issue, U.S. National Tsunami Hazard Mitigation Program.* — 2005. — Vol. 35, No. 1. — P. 41–58.
- [6] Baba T., Cummins Ph.R., Hong Kie Thio, Tsushima H. Validation and joint inversion of teleseismic waveforms for earthquake source models using deep ocean bottom pressure records: a case study of the 2006 Kuril megathrust earthquake // *Pure and Applied Geophysics.* — 2009. — Vol. 166, No. 1–2. — P. 55–76.
- [7] Percival D.B., Denbo D.W., Eble M.C., Gica E., Mofjeld H.O., Spillane M.C., Tang L., Titov V.V. Extraction of tsunami source coefficients via inversion of DARTr buoy data // *Nat. Hazards.* — 2011. — Vol. 58. — P. 567–590.
- [8] Tsushima H.R., Hino Y., Tamioka F., Imamura, Fujimoto H. Tsunami waveform inversion incorporating permanent seafloor deformation and its application to tsunami forecasting // *L. Geophys. Res.* — 2012. — Vol. 117, doi:10.1029/2011lb008877.

- [9] Wei Yo., Newman A., Hayes G. et al. Tsunami forecast by joint inversion of real-time tsunami waveforms and seismic or GPS data: application to the Tohoku 2011 tsunami // *Pure and Appl. Geoph.* — 2014. — Vol. 171, Iss. 12. — P. 3281–3305.
- [10] Mulia I.E., Asano T. Initial tsunami source estimation by inversion with an intelligent selection of model parameters and time delays // *J. Geophys. Res. Oceans.* — 2016. — Vol. 121, doi:10.1002/jgrc.21401.
- [11] Mungov G., Eblé M., Boucharde R. DART® tsunameter retrospective and real-time data: a reflection on 10 years of processing in support of tsunami research and operations // *Pure Appl. Geophys.* — 2013. — Vol. 170, Iss. 9. — P. 1369–1384.
- [12] Cheverda V.A., Kostin V.I. r -pseudoinverse for compact operator // *Siberian Electronic Mathematical Reports.* — 2010. — Vol. 7. — P. 258–282.
- [13] Voronina T.A., Tcheverda V.A. Reconstruction of tsunami initial form via level oscillation // *Bull. Novosibirsk Comp. Center. Ser. Math. Model. in Geoph.* — Novosibirsk, 1998. — Iss. 4. — P. 127–136.
- [14] Voronina T.A. Reconstruction of initial tsunami waveforms by a truncated SVD method // *J. Inverse and Ill-posed Problems.* — 2012. — Vol. 19. — P. 615–629.
- [15] Voronina T.A., Tcheverda V.A., Voronin V.V. Some properties of the inverse operator for a tsunami source recovery // *Siberian Electronic Mathematical Reports.* — 2014. — Vol. 11. — P. 532–547.
- [16] Voronin V.V., Voronina T.A., Tcheverda V.A. Inversion method for initial tsunami waveform reconstruction // *Nat. Hazards Earth Syst. Sci.* — 2015. — Vol. 15. — P. 1251–1263.
- [17] Lavrentiev M.M., Romanenko A.A., Lysakov K.F. Modern computer architecture to speed-up calculation of tsunami wave propagation // *Proc. XIth (2014) Pacific/Asia Offshore Mech. Symp. Shanghai, China, October 12–16, ISSN 1946-004X.* — 2014. — P. 186–191.